Deep-Sea Research I 56 (2009) 1727–1741

Contents lists available at ScienceDirect

Deep-Sea Research I

journal homepage: www.elsevier.com/locate/dsri

Impact of drifting icebergs on surface phytoplankton biomass in the Southern Ocean: Ocean colour remote sensing and *in situ* iceberg tracking

J.N. Schwarz *, M.P. Schodlok [1]

Climate Systems, Alfred Wegener Institute for Polar & Marine Research, Postfach 12 0161, 27515 Bremerhaven, Germany

ARTICLE INFO

Article history:
Received 23 April 2008
Received in revised form
28 April 2009
Accepted 5 May 2009
Available online 10 May 2009

Keywords:
Southern Ocean
Weddell Sea
Icebergs
Phytoplankton
Remote sensing

ABSTRACT

Icebergs that calve from the Antarctic ice shelves and drift in the Southern Ocean melt to deliver fresh water, dust and minerogenic particles to the surface ocean along the iceberg's path. Each of these components may have an effect on growth conditions for phytoplankton, as might the mechanical effects of the iceberg keel disturbing the water. Although anecdotal and small-scale surveys suggest that drifting icebergs increase local primary production, no large-scale studies have been reported. An analysis of satellite and automated iceberg tracking data from the Weddell Sea, covering the months October to March, from 1999 to 2004, showed that the probability of increased surface phytoplankton biomass was up to one-third higher in the wake of a tracked iceberg compared to background biomass fluctuations. Only during the month of February were the effects of icebergs on surface biomass likely to be negative, whereas background biomass fluctuations were likely to be negative during March. These results confirm icebergs as a factor affecting phytoplankton in the Southern Ocean and highlight the need for detailed process studies so that responses to future changes in the Antarctic ice sheets may be predicted.

1. Introduction

Anecdotal evidence has, for many years, suggested a link between the presence or passage of icebergs and enhanced phytoplankton growth in the Southern Ocean (Smetacek et al., 2002; Sachs, 2008). There are several mechanisms by which icebergs could be thought to improve the growth environment, but also several potential negative impacts. Furthermore, a particular physical process associated with an iceberg may have varying impacts, depending on the oceanic (Jansen et al., 2007) and ecological (Sullivan et al., 1993) conditions through which it is passing. For example, an iceberg with a deep keel, passing through deeply mixed waters, could mix micronutrients from below the pycnocline into the surface and also, by shedding meltwater at the waterline, alter the density structure of the upper water column. In the absence of strong wind-driven mixing, the iceberg meltwater would form a stable lens of low-salinity water in which phytoplankton cells are bathed in sunlight, resulting in an increase in surface phytoplankton biomass. The same processes acting on different initial conditions, such as a well-stratified water column with high phytoplankton biomass in the upper layer, could produce the contrary effects of diluting the surface phytoplankton population through mixing and slowing growth by destroying the stable surface layer and thus forcing cells

* Corresponding author. Now at: National Institute for Water & Atmosphere Research, 301 Evans Bay Parade, Kilbirnie, Wellington 6021, New Zealand. Tel: +64 4 386 0591.
E-mail address: j.schwarz@niwa.co.nz (J.N. Schwarz).
[1] Now at: Jet Propulsion Laboratory, California Institute of Technology, MS 300-323, 4800 Oak Grove Drive, Pasadena, CA 91109-8099, USA.

0967-0637/$ - see front matter © 2009 Elsevier Ltd. All rights reserved.
doi:10.1016/j.dsr.2009.05.003

to adapt to lower light levels. The individual processes can be summarised in two groups: mechanical disturbance and melting.

1.1. Mechanical disturbance

Surveys of iceberg size indicate that typical keel depths for medium-sized icebergs (dimensions of the order of 1 km) range between 140 and 600 m at the time of calving (Dowdeswell and Bamber, 2007). Near the coast, this may be sufficient for the berg to be grounded, potentially disturbing circulation patterns, sea-ice formation and consequently the entire ecosystem (Arrigo et al., 2002). The case of grounded icebergs is not further discussed in this paper. Once an iceberg is adrift, the keel causes turbulent mixing, potentially enabling transfer of thermal energy, nutrients, phytoplankton cells and water of different salinity across the pycnocline (the base of the mixed layer). The degree of turbulence is determined by the topography of the iceberg's keel and by the relative velocities of the iceberg and the surrounding water. Upwelling of macro-nutrients (nitrate, phosphate, silicate) would be likely to have a positive impact on phytoplankton growth in the summer season, if the surface waters are stratified, with a shallow surface mixed layer (30 to 50 m) in which nitrate and silicate are depleted (Dafner et al., 2003). Input of micro-nutrients (specifically iron) is likely to promote phytoplankton growth in the summer and in any season with sufficient light for growth in the high-nutrient/low-chlorophyll (HNLC) regions (Martin et al., 1991; Holm-Hansen and Hewes, 2004). Conversely, a high concentration of phytoplankton cells near the ocean surface could also be reduced as it is mixed downward through the water column by the passing iceberg. Surface chlorophyll concentrations, as monitored by satellite-borne detectors, would then decrease. Whether cells are actually lost from the mixed layer would depend on the iceberg keel depth, which dictates the degree of turbulent mixing relative to the mixed layer depth. The mixed layer may become deeper as a result of the iceberg's passage, in which case cells could be retained within the mixed layer, but be more deeply mixed.

1.2. Melting

Smith et al. (2007) reported the presence of slightly reduced salinities surrounding two icebergs close to the Antarctic Peninsula. Oceanic water layers are ordered according to density gradients, which are determined by both temperature and salinity. The net effect of melt water on the water column structure depends on the volume of water melting, the strength of wind-mixing, the ambient temperature and the ambient salinity structure: Unless the ambient temperature is close to freezing, the melt water will have a negative temperature component of buoyancy, while the salinity component will be positive, since fresh water is less dense than saline water. Any positive increase in density gradient caused by the input of freshwater must then withstand the physical mixing effect of the wind, or the new stratification will be destroyed. The melt water lens alleviates light limitation for cells trapped within it (e.g. Lancelot et al., 1993; Mitchell and Holm-Hansen, 1991). In contrast, input of melt water at depth is likely to result in upwelling of water from below the thermocline, bringing nutrients into the surface mixed layer (Jenkins, 1999).

The glaciers from which icebergs calve also accumulate dust, which falls with snow, over many thousands of years. Although Antarctica is too isolated at present to receive large inputs of aeolian dust, this has not always been the case: The deposition rate of dissolvable iron within dust in East Antarctica has been found to be a factor of two greater during interglacial than glacial periods (Edwards et al., 2006). Concentrations of dissolvable iron in modern snow deposited on sea-ice in the same region have been reported to reach 23.7 nM, compared to ambient concentrations of below 4.5 nM below sea-ice and less than 1 nM in the open Southern Ocean (Lannuzel et al., 2007; de Baar, 1995; de Baar et al., 1999). As an iceberg melts and breaks up, the entire accumulated stock of iron is released into the surrounding water at a range of depths up to the keel depth. Massive colonies of algae have been observed to be resident on drifting icebergs (Smith et al., 2007). These cells could alter the phytoplankton community composition of waters in which they are shed as melting proceeds, potentially out-competing the prevailing species.

While several theoretical studies have examined the fluid dynamics of iceberg melting and turbulence (Jenkins, 1999; Huppert, 1980), none has yet sought to prove or disprove the hypothesis that drifting icebergs consistently have a marked impact on the food chain. The problems of modelling physical, chemical and biological processes in detail around an iceberg are many and various: The iceberg topography must be accurately simulated and melting, erosion and turbulence realistically implemented at high spatial resolution. Data to initiate such a model are scarce, and sufficient data to validate it are not known to exist. In the field, only one oceanographic survey has yet dedicated sufficient time and resources to address these problems: Over a period of three weeks, two icebergs off the Antarctic Peninsula were observed in great detail and were found to support considerable populations of phyto- and zooplankton (Smith et al., 2007). Many more ship hours would be required to gather a statistically significant sampling of icebergs in all the conditions encountered in the Southern Ocean. An alternative means to modelling or *in situ* sampling is offered by satellite remote-sensing (Marrari et al., 2006): If iceberg positions are accurately recorded, then records of surface chlorophyll concentration derived from satellite data can be consulted to determine whether the concentration before an iceberg transits a given location was higher or lower than the concentration afterwards. Remote sensing does not provide an ideal data set: Chlorophyll-a in the surface layer (down to approximately 1 optical depth, which is typically ~10 m in these waters, Gordon and McCluney, 1975), is currently retrieved with an accuracy of ±33% using a global algorithm (O'Reilly et al., 1998; Bailey and Werdell, 2006). Surface chlorophyll has been found to be generally well-correlated with the depth-integrated value in open ocean waters (Morel and Berthon, 1989), with some natural variability (Uitz et al., 2006 reported correlation coefficients greater than 0.7, $n > 58$, between chlorophyll concentrations within the first optical penetration depth and the euphotic zone for mixed and stratified waters). However, in some locations, including large swaths of high latitude waters, deep chlorophyll maxima (DCM) are found with no correlation between the surface and depth-integrated values (e.g. Holm-Hansen and Hewes, 2004; Hill et al., 2008). In the context of icebergs altering the growth environment, a DCM could be disturbed by the passage of an iceberg, resulting in an undetected loss of 'invisible' biomass from the pycnocline, or the deep community could lose their light source in the event that a new population grows above it in a meltwater lens, resulting in an apparent (and possibly false) net gain in biomass, caused by the iceberg. In this latter case, the biomass of the meltwater population may or may not exceed that of the DCM. Despite these limitations, remote sensing is the only source of large-scale, synoptic estimates of chlorophyll-a. Keeping in mind that remote sensing detects only the surface phytoplankton population, this study tests the null hypothesis that:

> 'An iceberg has no significant impact on the ambient surface chlorophyll dynamics.'

2. Methods

2.1. Iceberg tracks

For the past 9 years, tracking beacons have been deployed on medium-sized icebergs, defined as those with length dimensions on the order of 1 km, as part of a physical oceanography research program at the Alfred Wegener Institute. Icebergs of this size are not routinely monitored by the National Snow and Ice Data Centre. Latitude and longitude, together with some ancillary data, are transmitted from each beacon via the ARGOS satellite system each day at 12 UTC. The current iceberg tracking dataset comprises 77 records, each covering periods from months up to three years, depending on the lifetime of the tracked iceberg. Full details can be found in Schodlok et al. (2006).

2.2. Satellite surface chlorophyll-a

Satellite ocean colour data were processed and analysed in four steps, detailed in Sections 2.2.1–2.2.4 below:

1. Producing suitable daily chlorophyll maps;
2. Extracting chlorophyll data at known iceberg locations;
3. Calculating the impact of the iceberg passage on surface chlorophyll;
4. Addressing uncertainties.

2.2.1. Chlorophyll maps

Firstly, surface chlorophyll concentrations were generated from Level 2 SeaWiFS data (oceancolor.gsfc.nasa.gov), mapped to 1 km resolution and combined into daily composites using the SeaDAS software v5.2 (seadas.gsfc.nasa.gov). Chlorophyll values below $1\times10^{-3}\,\mathrm{mg\,m^{-3}}$ and greater than $32\,\mathrm{mg\,m^{-3}}$ were excluded from further analysis as being outside the proven range of the satellite chlorophyll algorithms (O'Reilly et al., 1998).

2.2.2. Chlorophyll values along known iceberg tracks

Secondly, chlorophyll concentrations at every reported iceberg location were extracted from the ten-year chlorophyll record, regardless of whether the date on which an iceberg occupied a given location matched the date of the chlorophyll record.

2.2.3. Impact of iceberg passage on surface chlorophyll

Two 6-day means of satellite-derived chlorophyll were calculated for each pixel occupied by a tracked iceberg: For a given pixel along a known iceberg track, $\langle \mathrm{chl}^{i}_{\mathrm{before}} \rangle$ denotes the mean value in the 6 days prior to the iceberg's passage of the pixel, and $\langle \mathrm{chl}^{i}_{\mathrm{after}} \rangle$ denotes the mean value in the 6 days after the iceberg's passage. Owing to the high degree of cloudiness in the Southern Ocean, these mean values were typically calculated from between 1 and 3 cloud-free data points. The difference between these two values was calculated to give the change in surface chlorophyll following the iceberg's passage, $\Delta\mathrm{chl}^{i}$:

$$\Delta\mathrm{chl}^{i} = \langle \mathrm{chl}^{i}{}_{\mathrm{before}} \rangle - \langle \mathrm{chl}^{i}{}_{\mathrm{after}} \rangle \tag{1}$$

where the superscript i indicates a temporal match-up between a known iceberg passage and the satellite chlorophyll retrieval. Fig. 1 demonstrates the methodological concept, together with some of its drawbacks, using an iceberg tracked during January, 2003.

On January 6th, 2003, iceberg number 14958_5 passed through location -70.6902°N, -11.4972°E. Chlorophyll maps for 3 days prior to and 2 days after 6th January are shown in the left-hand column of Fig. 1, with the iceberg's known location on 6th January marked by a black circle. To facilitate plotting, the satellite chlorophyll data were processed into a standard mapped format. This generated some spuriously high values apparent in Fig. 1 as speckle. Note that the analysis of chlorophyll concentrations was carried out using the 6-day means of SeaWiFS level 3 chlorophyll data limited to $0.001–32\,\mathrm{mg\,m^{-3}}$, in which speckle was not observed. Throughout the rest of the paper, all mentions of 'chlorophyll' refer to 6-day means of satellite-derived surface chlorophyll-a.

The middle column of Fig. 1 shows the top-of-atmosphere radiance from channel 1 (processing Level 1A, 645 nm, 250×250 m resolution) from MODIS-Aqua, for the same dates as the SeaWiFS images in the left-hand column. The colour-scale has been set to emphasize the contrast between ice and water, so that no detail is visible across the open water surfaces. A red circle marks the location occupied by the iceberg on 6th January. The third column of Fig. 1 shows a zoomed-in version of the 645 nm channel data, with the iceberg location on each date marked by a yellow square. It is evident that many more icebergs are present, at least within the first 5° of latitude adjacent to the Antarctic coast, than are, or realistically can be, tracked. These represent a potential influence on

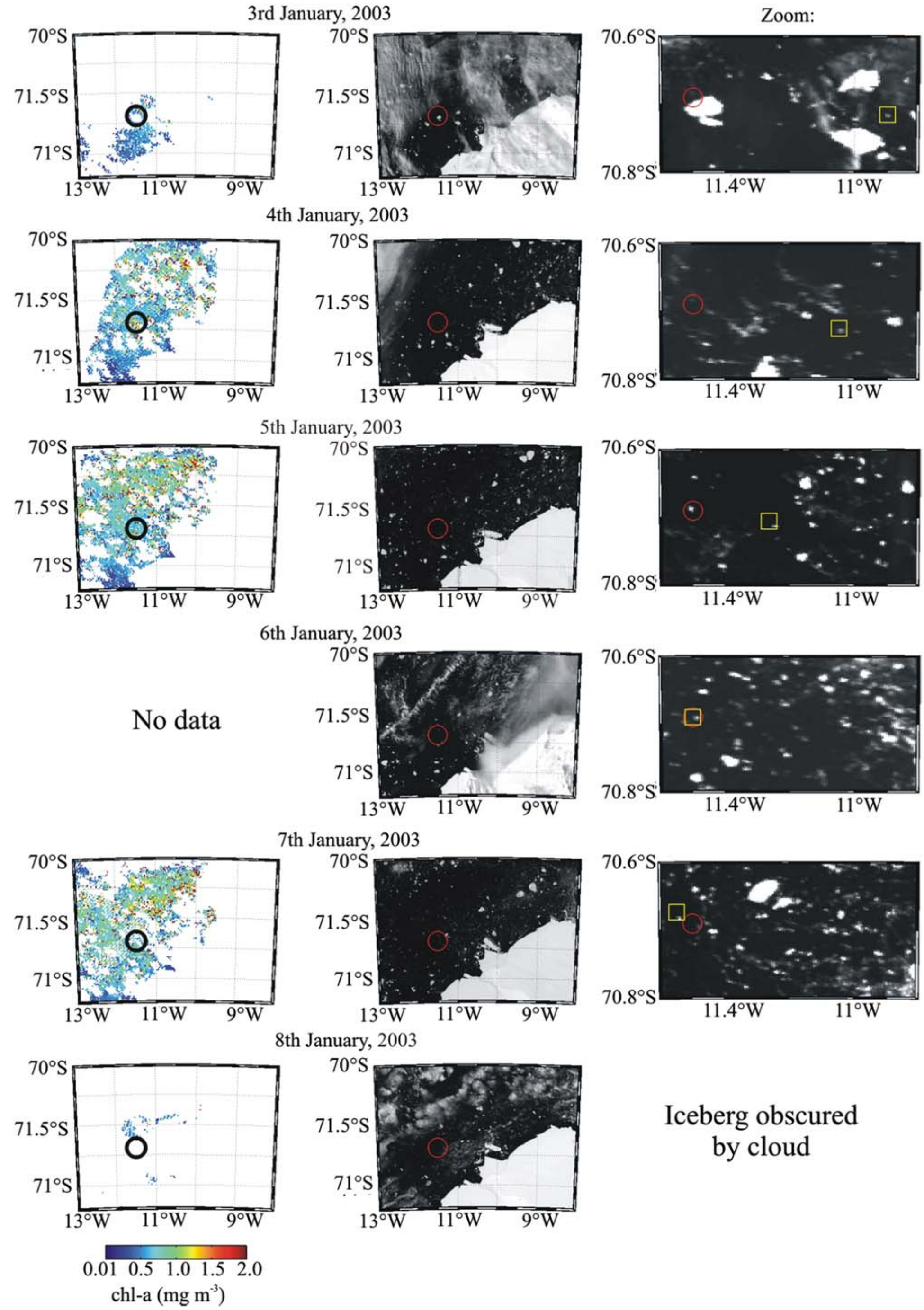

Fig. 1. Demonstration of the methodology. First column: surface chlorophyll concentrations derived from SeaWiFS imagery from 3rd to 8th January, 2003, over a section of the Antarctic mainland and Weddell Sea; pixel of interest is ringed in black, white denotes pixels excluded because of contamination or obscuration by clouds or ice. Iceberg '14958_5', with dimensions of $\sim 380 \times 380$ m, occupied the pixel of interest on 6th January, 2003. Second column: 250 m resolution images derived from channel 1 top-of-atmosphere radiance from MODIS-Aqua (Level 1A, 645 nm, 250×250 m resolution). The Antarctic continental ice sheets and drifting icebergs appear white, while cloud cover appears puffy and grey and water appears black. The pixel of interest is ringed in red. Third column: As second column but zoomed in to show the pixel of interest (red circle) as well as iceberg '14958_5' (yellow squares indicate the iceberg location at 12 UTC each day). Since the time at which the satellite images were collected is between 30 minutes and 3 hours earlier than the time at which iceberg location was recorded, the iceberg is not always in the centre of the yellow square. The mean of valid chlorophyll values at the pixel of interest during the 6 days prior to 6th January, 2003 provides the $\langle \mathrm{chl}^{\mathrm{i}}_{\mathrm{before}} \rangle$ value, while the means of chlorophyll at the pixel of interest over 6 day intervals at any other time in the satellite record provide values of $\langle \mathrm{chl}^{\mathrm{ni}}_{\mathrm{before}} \rangle$. Similarly, the mean chlorophyll value from 7th to 12th January, 2003 gives $\langle \mathrm{chl}^{\mathrm{i}}_{\mathrm{after}} \rangle$.

chlorophyll concentrations that can not be accounted for directly.

2.2.4. Impact of factors other than a tracked iceberg on chlorophyll

In order to evaluate the effects of a tracked iceberg on surface chlorophyll, the effects of other factors on chlorophyll must be considered. These factors include untracked icebergs, as mentioned in Section 2.2.3, as well as wind- and current-driven mixing, advection, ambient phytoplankton growth dynamics, grazing and bacterial or viral infection of the phytoplankton population, errors in the retrieved chlorophyll concentrations and contamination of the satellite signal by sub-pixel clouds and ice not picked up by the processing routines. To account for these factors, the change in chlorophyll between two successive 6-day periods was calculated as in Section 2.2.3, but considering only those times when it was known that no tracked iceberg transited each location. This produced a second dataset of changes in chlorophyll:

$$\Delta \mathrm{chl}^{\mathrm{ni}} = \langle \mathrm{chl}^{\mathrm{ni}}_{\mathrm{before}} \rangle - \langle \mathrm{chl}^{\mathrm{ni}}_{\mathrm{after}} \rangle \quad (2)$$

where the superscript ni denotes the case where no tracked iceberg passed the location. This dataset is referred to henceforth as the background dataset. The background dataset is drawn from the same iceberg paths as the main dataset, but includes many more locations along those paths.

2.3. Statistical testing

Statistical testing was required to test the null hypothesis that

> 'An iceberg has no significant impact on the ambient surface chlorophyll dynamics.'

In terms of the 6-day mean chlorophyll differences calculated as in Section 2.2, this can be expressed as:

> 'The sample dataset $\Delta \mathrm{chl}^{\mathrm{i}}$ is drawn from the background dataset $\Delta \mathrm{chl}^{\mathrm{ni}}$.'

Tests to detect differences in sample populations fall broadly into those that assume that both samples are normally distributed (parametric tests, e.g. *t*-test, Wilcoxon signed-rank test) and those that do not assume normal distribution (non-parametric tests, e.g. Wald-Wolfowitz runs test, Mann-Whitney *U*-test, two-sample Kolmogorov –Smirnov test). For the non-parametric tests, it is assumed that the two samples, although not normally distributed, do come from the same distribution, and different tests have varying sensitivity to this assumption. The null hypothesis above states that the iceberg sample data are a subsample of the background dataset, which clearly implies that the two samples share a sample distribution. Since the null hypothesis states that the iceberg passage has no affect on chlorophyll, it should not be possible, if the null hypothesis is true, that the two sample sets will have different variances. However, to be sure that the test sample set does not simply exhibit a different variance because it is sparsely sampled, the possibility that the null hypothesis is true and the sample sets have different variances should be considered. To select a test for the null hypothesis, it must therefore be determined:

(a) whether the two sample sets are normally distributed;
(b) whether the two sub-samples are equally distributed.

Point (a) can be determined using a simple normality test, of which there are many. The Jarque-Bera test was chosen here because it is not overly sensitive to the tails of the distribution (where the $\Delta \mathrm{chl}^{\mathrm{i}}$ sample set is rather sparse) and is not adversely affected by large sample sizes, as is the more powerful Shapiro-Wilkes test. Since chlorophyll distributions are typically log-normally distributed (Campbell, 1995), both Δchl datasets were also recalculated using log-transformed $\langle \mathrm{chl}^{\mathrm{ni/i}}_{\mathrm{after/before}} \rangle$ and re-tested for normality.

Depending on the Δchl distributions, point (b) requires either parametric or non-parametric tests that:

- allow unequal sample sizes;
- assume equal variances;
- are not affected by large sample sizes, and
- are sensitive to differences in the underlying distributions.

An additional step should remove the fourth constraint, and allow for different variances of the two sample sets. The tests chosen subject to these conditions were:

1. *F*-test for equal variances;
2. *t*-test for normally distributed, independent datasets with equal variance;
3. *t*-test for normally distributed, independent datasets with different variances (equivalent to the Behrens-Fisher test);
4. Mann-Whitney-Wilcoxon test for equally, but not normally distributed datasets;
   To our knowledge, there is no non-parametric test of differences between populations which do not share a distribution. The test results are discussed and compared in detail in Section 3. To quantify the difference a passing iceberg has on surface chlorophyll, a further technique was applied:
5. Hodges-Lehmann estimate of the median difference between $\Delta \mathrm{chl}^{\mathrm{i}}$ and $\Delta \mathrm{chl}^{\mathrm{ni}}$.

To reduce the calculation time for the Hodges-Lehmann estimate for such a large dataset, the median difference was calculated 100,000 times using random resamplings of a subset of datapoints from the large background dataset, each subtracted from the full iceberg dataset. The range and median of these differences are reported. Finally, it is conceivable that the impact of a passing iceberg is affected by the surface chlorophyll concentration that it encounters. This possibility was tested by partitioning the $\Delta \mathrm{chl}^{\mathrm{i/ni}}$ data into positive and negative values, and applying the Mann-Whitney-Wilcoxon test to ascertain whether the $\langle \mathrm{chl}^{\mathrm{i/ni}}_{\mathrm{before}} \rangle$ values in each data partition were significantly different to one another. Statistical tests were chosen based on information in Wikipedia, Matlab and Lyons (1991).

3. Results and discussion

Satellite-derived chlorophyll concentrations within 6 days both before and after transit of the iceberg across a given location were found in 215 instances, involving 24 of the 77 tracked icebergs. Details are given in Table 1. The background chlorophyll data set of locations along known iceberg paths at times when no iceberg was present comprised 690,444 data points. A Jarque-Bera test showed that neither the background nor the matchup datasets were normally distributed ($\alpha = 0.01$, $p < 0.01$, $N = 690{,}444$ and 215 for the background and matchup datasets, respectively). Log-transformation of $\langle \mathrm{chl} \rangle$ prior to calculation of Δchl produced bell-shaped but non-normal distributions in both cases. Table 2 summarises the statistics of both datasets.

Trends in Δchl are shown in Fig. 2. The monthly background $\Delta \mathrm{chl}^{\mathrm{ni}}$ data reflect ambient growth dynamics along the iceberg paths. That is, chlorophyll generally increased each month from October to February and decreased in March. Median values of $\Delta \mathrm{chl}^{\mathrm{i}}$, where an iceberg transit was recorded, were positive and around an order of magnitude higher than those of $\Delta \mathrm{chl}^{\mathrm{ni}}$ for the full dataset and also for the individual months of November, December and January. The maximum Δchl values were observed during November for both iceberg and no-iceberg datasets. This corresponds to the season of rapid sea-ice retreat (e.g. Smith and Comiso, 2008) so phytoplankton growth can be supported both by sea-ice meltwater lens formation (Smith, 1985) and by increased light availability. Under these conditions, the net positive impact of iceberg transit could be attributed to upwelling of micronutrients but, for this to be the case, any supply of iron from melting sea-ice must be rapidly exhausted. In February, the background dataset tended toward low but positive values of $\Delta \mathrm{chl}^{\mathrm{ni}}$, whereas $\Delta \mathrm{chl}^{\mathrm{i}}$ tended to be negative. Seasonal sea-ice cover has typically melted by February and insolation is approaching the annual maximum, so that heating of the water, and associated thermal stratification, is strong. This may give rise to higher iceberg melt-rates, enhancing the formation of iceberg meltwater lenses and/or increasing the effects of mixing by the input of buoyant meltwater deeper in the water column and by the passage of the iceberg keel itself. Given high accumulated phytoplankton stocks in well-stratified water, these effects would combine to cause an apparent decrease in surface chlorophyll by dilution. In March, few iceberg matchup-points were found ($N = 8$), but for these points $\Delta \mathrm{chl}^{\mathrm{i}}$ and $\Delta \mathrm{chl}^{\mathrm{ni}}$ were roughly equal in magnitude but negative for $\Delta \mathrm{chl}^{\mathrm{ni}}$, positive for $\Delta \mathrm{chl}^{\mathrm{i}}$. This would suggest that once phytoplankton growth is generally in decline at the onset of austral autumn, an iceberg transit replenishes nutrients and thereby promotes growth. It would also be possible that an iceberg meltwater lens restabilises the water column if wind mixing has increased at the onset of autumn. However, more data are required for this late summer period before firm conclusions can be drawn.

Statistical tests to establish whether the two datasets – $\Delta \mathrm{chl}^{\mathrm{i}}$ and $\Delta \mathrm{chl}^{\mathrm{ni}}$ – were distinctive, were contradictory, with two tests indicating that the distributions are indeed different, and another test failing to reject any hypotheses:

- The *F*-test for unequal variances confirmed that the two distributions have different variances ($p < 1 \times 10^{-8}$).
- The 2-way *t*-test failed to reject any of three contradictory hypotheses at the $\alpha = 0.01$ significance level. The hypotheses were that the mean of $\Delta \mathrm{chl}^{\mathrm{i}}$ is identical to the mean of $\Delta \mathrm{chl}^{\mathrm{ni}}$ ($p = 0.26$); that the mean $\Delta \mathrm{chl}^{\mathrm{i}}$ is greater than the mean $\Delta \mathrm{chl}^{\mathrm{ni}}$ ($p = 0.0625$) and that the mean $\Delta \mathrm{chl}^{\mathrm{i}}$ is less than the mean $\Delta \mathrm{chl}^{\mathrm{ni}}$ ($p = 0.9375$).
- The (non-parametric) Mann-Whitney-Wilcoxon test rejected the hypothesis that $\Delta \mathrm{chl}^{\mathrm{i}}$ and $\Delta \mathrm{chl}^{\mathrm{ni}}$ are non-normally distributed datasets with equal medians ($p < 1 \times 10^{-6}$).
- The Hodges-Lehmann estimate of the median difference between $\Delta \mathrm{chl}^{\mathrm{i}}$ and $\Delta \mathrm{chl}^{\mathrm{ni}}$ returned a value of $0.1003 \pm 0.0311\,\mathrm{mg\,m^{-3}}$ (± 1 standard deviation), with a range of -0.0151 to $0.2622\,\mathrm{mg\,m^{-3}}$, i.e. $\Delta \mathrm{chl}^{\mathrm{i}}$ exceeded $\Delta \mathrm{chl}^{\mathrm{ni}}$.
- For individual months, differences between the $\Delta \mathrm{chl}^{\mathrm{i}}$ and $\Delta \mathrm{chl}^{\mathrm{ni}}$ datasets were significant for November to January (Mann-Whitney-Wilcoxon test, $\alpha = 0.01$, p and N values given in Table 2).

Given the agreement of the Mann-Whitney-Wilcoxon test with the Hodges-Lehmann estimation of a positive median difference between the iceberg and background datasets, it seems likely that the inconclusive *t*-tests can be attributed to the large difference in the dataset sizes. The range in the Hodges-Lehmann estimate is consistent with direct comparisons of monthly Δchl values shown in Table 2.

The Mann-Whitney-Wilcoxon test confirmed significant positive differences between $\Delta \mathrm{chl}^{\mathrm{i}}$ and $\Delta \mathrm{chl}^{\mathrm{ni}}$ data for the period from November to January, i.e. the main growth season. Median Δchl values for these months were up to 2 orders of magnitude greater in the presence of an iceberg, but note that variability was high for both datasets (Table 2).

It is conceivable that the surface biomass at the time of an iceberg transit determines the effect that the iceberg has. For example, high surface chlorophyll concentrations may be associated with nutrient depletion, so that nutrients mixed into the surface by iceberg-induced turbulence, whether by meltwater rising from the keel or from direct mixing by the keel itself, relieve nutrient limitation and result in an increase in surface biomass because of increased phytoplankton growth. Equally, a high surface chlorophyll concentration could be indicative of high stratification, so that iceberg-induced mixing is likely to mix the surface population down to greater depths, causing an apparent loss of surface biomass.

To investigate possible links between initial chlorophyll concentration and the apparent impact of the

Table 1
Details of tracked icebergs occupying locations at times for which valid chlorophyll data were available within 6 days both before and after the iceberg passed through.

Year	Month	Day	Latitude	Longitude	Before iceberg transit		After iceberg transit		Δchl^i	Iceberg tag
					$\langle chl^i_{before} \rangle$	No. obs.	$\langle chl^i_{after} \rangle$	No. obs.		
2001	1	24	−61.0171	−19.881	0.132	1	0.095	1	−0.037	14954_2
2003	2	17	−68.6641	13.1109	0.119	2	0.111	1	−0.007	14954_5
2003	2	25	−68.3875	12.5737	0.121	1	0.145	2	0.024	14954_5
2003	2	26	−68.4499	12.7889	0.098	1	0.125	1	0.027	14954_5
2003	1	11	−69.2953	−2.0388	0.901	1	1.619	1	0.717	14956_5
2003	1	12	−69.4004	−2.1754	1.088	1	1.576	1	0.488	14956_5
2004	1	19	−65.6941	−18.5354	0.127	2	0.112	1	−0.015	14956_5
2004	1	20	−65.6988	−18.5911	0.127	2	0.112	1	−0.015	14956_5
2004	1	21	−65.6798	−18.6952	0.127	2	0.112	1	−0.015	14956_5
2004	1	22	−65.6949	−18.8024	0.130	1	0.112	1	−0.018	14956_5
2003	1	6	−70.6902	−11.4972	0.521	1	0.494	1	−0.027	14958_5
2003	1	7	−70.6737	−11.5448	0.510	3	1.424	1	0.914	14958_5
2003	1	8	−70.5224	−11.6238	0.585	1	1.492	1	0.906	14958_5
2003	1	10	−70.6045	−12.3569	0.824	2	0.747	1	−0.077	14958_5
2003	1	11	−70.585	−12.694	0.752	1	1.366	2	0.615	14958_5
2003	1	12	−70.5225	−12.758	0.806	1	1.535	2	0.729	14958_5
2003	1	14	−70.5185	−13.4071	0.764	1	3.036	1	2.272	14958_5
2003	1	15	−70.5913	−13.6893	1.192	1	2.274	2	1.082	14958_5
2003	1	16	−70.7224	−13.8491	0.544	1	1.467	3	0.922	14958_5
2003	1	17	−70.8358	-13.8317	1.451	1	1.365	3	−0.086	14958_5
2003	1	19	−71.0207	−13.7714	1.717	2	1.686	1	−0.031	14958_5
2003	1	20	−71.08	−13.9435	1.875	2	1.649	1	−0.226	14958_5
2003	2	2	−72.0087	−16.5601	11.371	1	0.849	1	−10.521	14958_5
2001	1	22	−62.3285	8.316	0.225	1	0.195	1	−0.030	14959_2
2001	1	23	−62.2543	8.174	0.153	1	0.202	1	0.050	14959_2
2003	1	5	−71.0613	−12.6226	0.249	1	0.511	1	0.262	14959_5
2003	1	7	−71.0823	−12.5839	0.249	1	1.465	1	1.216	14959_5
2003	1	8	−71.0764	−12.5872	0.249	1	1.465	1	1.216	14959_5
2003	1	9	−71.0672	−12.5877	0.511	1	1.465	1	0.954	14959_5
2003	1	10	−71.0688	−12.5769	0.511	1	1.465	1	0.954	14959_5
2003	1	11	−71.0845	−12.6416	0.784	1	1.437	2	0.653	14959_5
2003	1	12	−71.0997	−12.8119	0.593	1	1.789	3	1.196	14959_5
2003	1	14	−71.0784	−13.1939	1.008	2	1.287	1	0.278	14959_5
2003	1	15	−71.1045	−13.2348	0.648	1	1.777	1	1.129	14959_5
2003	1	20	−71.2122	−13.8108	1.613	2	1.307	1	−0.306	14959_5
2003	1	21	−71.2344	−14.0482	1.998	2	1.823	1	−0.174	14959_5
2003	1	22	−71.2642	−14.3873	1.798	2	1.175	1	−0.623	14959_5
2003	1	27	−71.5084	−14.871	4.280	1	1.828	1	−2.452	14959_5
2003	1	28	−71.6401	−15.2447	1.236	1	0.256	1	−0.981	14959_5
2003	1	5	−70.9738	−13.5362	0.519	1	0.972	1	0.453	14960_5
2003	1	6	−71.0975	−13.6491	0.386	1	0.544	1	0.158	14960_5
2003	1	9	−71.0702	−14.7987	0.385	2	1.139	1	0.755	14960_5
2003	1	10	−71.1777	−15.1463	0.531	1	0.612	1	0.081	14960_5
2003	1	14	−71.376	−15.3313	0.665	1	2.463	2	1.799	14960_5
2003	1	15	−71.436	−15.2477	0.760	1	1.655	3	0.895	14960_5
2003	1	19	−71.561	−16.1905	1.059	2	2.217	1	1.158	14960_5
2003	1	20	−71.5778	−16.4063	1.381	2	1.856	1	0.475	14960_5
2003	1	24	−71.7133	−17.0847	1.078	1	0.794	1	−0.284	14960_5
2003	1	25	−71.717	−17.0891	1.078	1	0.794	1	−0.284	14960_5
2003	1	26	−71.7845	−17.2554	1.853	2	2.295	1	0.442	14960_5
2003	1	27	−71.9348	−17.4381	1.399	1	1.336	1	−0.063	14960_5
2003	2	25	−73.8468	−24.5554	0.595	1	0.208	1	−0.387	14960_5
2002	1	24	−66.2599	−16.6136	0.597	1	0.377	1	−0.219	25718_3
2002	1	25	−66.2751	−16.6959	0.597	1	0.375	1	−0.221	25718_3
2001	2	3	−68.9417	−7.5111	1.133	1	1.589	1	0.457	25826_3
2001	2	7	−69.1318	−8.1637	1.548	1	1.625	1	0.077	25826_3
2001	2	12	−69.287	−9.3895	1.778	1	1.138	1	−0.640	25826_3
2001	2	16	−69.3099	−10.0171	0.894	1	0.748	1	−0.146	25826_3
2004	1	24	−72.9863	−24.1908	1.806	1	3.097	1	1.291	25886_6
2002	2	21	−66.734	−19.1772	0.337	1	0.470	1	0.132	25887_3
2002	3	3	−66.8611	−20.3208	0.249	1	0.356	1	0.106	25887_3
2001	2	12	−67.3132	−1.4665	0.274	1	0.232	1	−0.042	25925_3
2003	1	10	−66.2195	0.4863	0.289	1	0.265	1	−0.024	8056_5
2003	1	10	−66.2899	0.3651	0.375	1	0.375	1	0.000	8056_5
2003	1	11	−66.3264	0.2513	0.375	1	0.375	1	0.000	8056_5
2003	1	11	−66.3361	0.1789	0.336	1	0.436	1	0.100	8056_5

Table 1 (*continued*)

Year	Month	Day	Latitude	Longitude	Before iceberg transit		After iceberg transit		Δchl^i	Iceberg tag
					$\langle chl^i_{before} \rangle$	No. obs.	$\langle chl^i_{after} \rangle$	No. obs.		
2003	1	12	−66.4369	−0.2293	0.296	1	0.354	1	0.058	8056_5
2003	1	12	−66.4534	−0.2681	0.306	1	0.554	1	0.249	8056_5
2003	12	26	−61.892	−45.891	0.284	2	2.235	1	1.952	8057_4
2003	12	27	−61.924	−45.89	0.362	1	2.235	1	1.874	8057_4
2004	3	12	−61.433	−43.089	0.167	1	0.186	1	0.020	8057_4
2004	3	21	−61.33	−42.627	0.265	1	0.098	1	−0.167	8057_4
2002	2	5	−66.883	−51.846	0.312	1	1.251	1	0.939	8061_4
2002	2	6	−66.95	−51.645	0.642	1	0.803	2	0.161	8061_4
2002	2	13	−67.329	−50.973	0.666	2	0.370	1	−0.296	8061_4
2002	2	14	−67.261	−50.857	0.769	1	0.536	1	−0.232	8061_4
2002	2	16	−67.138	−50.851	0.622	2	0.506	2	−0.116	8061_4
2002	2	17	−67.109	−50.925	0.904	1	0.369	2	−0.535	8061_4
2002	2	18	−67.092	−51.081	0.470	1	0.266	1	−0.204	8061_4
2002	2	19	−67.062	−51.178	0.337	1	0.347	2	0.010	8061_4
2002	2	20	−67.074	−51.236	0.337	1	0.343	1	0.006	8061_4
2002	10	17	−59.1111	−47.0803	0.083	1	0.185	1	0.103	8066_4
2003	2	10	−57.2539	−41.6439	0.108	1	0.146	1	0.038	8066_4
2003	2	10	−57.2461	−41.4644	0.145	1	0.138	1	−0.007	8066_4
2003	2	11	−57.2434	−41.3934	0.145	1	0.138	1	−0.007	8066_4
2003	2	18	−56.4798	−41.6772	0.131	1	0.125	1	−0.006	8066_4
2003	2	18	−56.4861	−41.6243	0.131	1	0.135	1	0.004	8066_4
2003	2	11	−51.8572	−38.281	0.467	1	0.948	1	0.481	8068_4
2003	2	12	−51.8622	−38.2642	0.467	1	0.948	1	0.481	8068_4
2001	10	3	−63.2668	−54.0432	0.151	1	0.152	2	0.002	8069_1
2001	10	4	−63.266	−54.0258	0.151	1	0.152	2	0.002	8069_1
2001	10	5	−63.2655	−54.031	0.129	2	0.152	2	0.023	8069_1
2001	10	6	−63.2657	−54.03	0.129	2	0.174	1	0.044	8069_1
2001	10	7	−63.2646	−54.03	0.129	2	0.174	1	0.044	8069_1
2001	10	9	−63.266	−54.0271	0.120	2	0.145	1	0.025	8069_1
2001	10	9	−63.2702	−54.0481	0.120	2	0.203	1	0.084	8069_1
2001	10	10	−63.2656	−54.0329	0.152	2	0.145	1	−0.007	8069_1
2001	10	10	−63.2685	−54.0309	0.152	2	0.203	1	0.051	8069_1
2001	10	11	−63.2645	−54.0288	0.152	2	0.145	1	−0.007	8069_1
2001	10	11	−63.2669	−54.0437	0.148	2	0.203	1	0.056	8069_1
2001	10	11	−63.268	−54.0367	0.152	2	0.203	1	0.051	8069_1
2001	10	12	−63.2653	−54.0263	0.152	2	0.145	1	−0.007	8069_1
2001	10	13	−63.2672	−54.0278	0.174	1	0.145	1	−0.029	8069_1
2001	10	13	−63.2643	−54.0311	0.174	1	0.203	2	0.029	8069_1
2001	10	14	−63.2652	−54.0331	0.174	1	0.261	1	0.087	8069_1
2001	10	17	−63.2633	−54.0369	0.145	1	0.261	1	0.116	8069_1
2001	11	6	−63.2661	−54.0363	0.097	1	0.296	1	0.199	8069_1
2001	11	6	−63.2753	−54.0466	0.193	1	0.298	1	0.105	8069_1
2001	11	7	−63.2661	−54.0343	0.097	1	0.296	1	0.199	8069_1
2001	11	8	−63.272	−54.0448	0.097	1	0.314	2	0.216	8069_1
2001	11	9	−63.2653	−54.0365	0.097	1	0.314	2	0.216	8069_1
2001	11	10	−63.2672	−54.0391	0.097	1	0.314	2	0.216	8069_1
2001	11	14	−63.2664	−54.029	0.298	1	0.593	1	0.295	8069_1
2001	11	14	−63.261	−54.0258	0.296	1	0.452	1	0.156	8069_1
2001	11	15	−63.2469	−54.0425	0.335	2	0.452	1	0.117	8069_1
2001	11	15	−63.259	−54.0518	0.314	2	0.452	1	0.139	8069_1
2001	11	15	−63.2548	−54.0422	0.335	2	0.452	1	0.117	8069_1
2001	11	15	−63.2595	−54.0052	0.336	2	0.593	1	0.257	8069_1
2001	11	15	−63.2648	−53.9676	0.347	2	0.593	1	0.246	8069_1
2001	11	16	−63.2396	−53.9987	0.335	2	0.452	1	0.117	8069_1
2001	11	16	−63.2699	−53.9707	0.347	2	0.593	1	0.246	8069_1
2001	11	16	−63.2975	-53.9141	0.298	1	0.593	1	0.295	8069_1
2001	11	17	−63.3288	−53.8787	0.355	1	0.670	1	0.314	8069_1
2001	11	17	−63.3575	−53.8535	0.355	1	0.780	1	0.424	8069_1
2001	11	17	−63.3746	−53.7807	0.517	2	2.177	1	1.660	8069_1
2001	11	17	−63.3626	−53.7208	0.517	2	1.359	2	0.842	8069_1
2001	11	17	−63.349	−53.6779	0.417	1	1.359	2	0.942	8069_1
2001	11	17	−63.3356	−53.6605	0.461	1	0.477	2	0.016	8069_1
2001	11	18	−63.3092	−53.771	0.470	1	0.729	1	0.259	8069_1
2001	11	18	−63.3347	−53.793	0.355	1	1.332	2	0.977	8069_1
2001	11	18	−63.3724	−53.7814	0.617	1	1.952	2	1.335	8069_1
2001	11	18	−63.3834	−53.7099	0.617	1	1.422	2	0.805	8069_1
2001	11	18	−63.3794	−53.6434	0.533	1	1.185	3	0.652	8069_1
2001	11	18	−63.3741	−53.5881	0.533	1	0.732	3	0.199	8069_1

Table 1 (*continued*)

Year	Month	Day	Latitude	Longitude	Before iceberg transit		After iceberg transit		Δchl^i	Iceberg tag
					$\langle chl^i_{before} \rangle$	No. obs.	$\langle chl^i_{after} \rangle$	No. obs.		
2001	11	18	−63.3665	−53.5609	0.528	1	0.647	3	0.119	8069_1
2001	11	19	−63.348	−53.5695	0.528	1	0.836	1	0.308	8069_1
2001	11	19	−63.3368	−53.5945	0.528	1	0.567	2	0.039	8069_1
2001	11	19	−63.3492	−53.596	0.528	1	0.574	3	0.046	8069_1
2001	11	19	−63.3749	−53.5661	0.528	1	0.712	2	0.184	8069_1
2001	11	19	−63.3971	−53.4883	0.483	1	1.700	2	1.217	8069_1
2001	11	19	−63.3922	−53.4011	0.483	1	3.009	2	2.525	8069_1
2001	11	19	−63.3848	−53.3242	0.517	1	1.394	1	0.877	8069_1
2001	11	19	−63.3607	−53.269	0.441	1	1.664	1	1.223	8069_1
2001	11	21	−63.383	−53.2662	1.271	1	1.664	1	0.393	8069_1
2001	11	24	−63.2933	−53.1968	0.393	2	0.715	1	0.322	8069_1
2001	11	25	−63.3331	−53.224	0.881	1	0.715	1	−0.166	8069_1
2001	11	26	−63.2983	−53.2309	0.541	1	0.404	1	−0.137	8069_1
2001	11	26	−63.2774	−53.2864	0.541	1	0.459	1	−0.082	8069_1
2001	11	26	−63.219	−53.2582	0.456	1	0.459	1	0.002	8069_1
2001	11	27	−63.1969	−53.2821	0.456	1	0.459	1	0.002	8069_1
2001	11	27	−63.1936	−53.3204	0.343	1	0.459	1	0.116	8069_1
2001	11	27	−63.2046	−53.3399	0.456	1	0.459	1	0.002	8069_1
2001	11	28	−63.226	−53.2685	0.456	1	0.459	1	0.002	8069_1
2001	11	28	−63.2349	−53.2973	0.348	1	0.459	1	0.111	8069_1
2001	11	28	−63.2539	−53.2549	0.541	1	0.459	1	−0.082	8069_1
2001	11	30	−63.3604	−52.9859	1.265	1	1.710	2	0.445	8069_1
2001	11	30	−63.4296	−52.85	4.668	1	1.574	2	−3.094	8069_1
2001	12	1	−63.4705	−52.7504	6.923	1	1.454	1	−5.469	8069_1
2001	12	2	−63.4595	−52.7012	6.923	1	1.454	1	−5.469	8069_1
2001	12	3	−63.5269	−52.4521	1.110	1	1.793	1	0.683	8069_1
2001	12	3	−63.5247	−52.515	0.272	1	1.793	1	1.521	8069_1
2001	12	3	−63.5882	−52.4817	0.958	1	1.144	1	0.187	8069_1
2001	12	3	−63.6133	−52.4059	0.958	1	1.211	1	0.253	8069_1
2001	12	3	−63.6133	−52.3863	0.970	1	1.211	1	0.241	8069_1
2001	12	4	−63.5925	−52.3979	0.958	1	1.144	1	0.187	8069_1
2001	12	4	−63.6127	−52.3221	0.970	1	1.718	2	0.748	8069_1
2001	12	4	−63.6264	−52.2752	0.970	1	2.226	1	1.256	8069_1
2001	12	5	−63.6189	−52.2822	0.970	1	3.597	2	2.627	8069_1
2001	12	6	−63.5666	−52.1401	0.765	1	2.145	2	1.380	8069_1
2001	12	6	−63.5431	−52.0994	1.347	1	12.209	1	10.862	8069_1
2001	12	7	−63.5469	−52.0693	1.101	2	1.167	1	0.066	8069_1
2001	12	7	−63.5283	−52.0795	1.166	2	12.209	1	11.043	8069_1
2001	12	7	−63.527	−52.0662	1.197	2	1.167	1	−0.030	8069_1
2001	12	7	−63.5257	−52.0471	1.101	2	1.167	1	0.066	8069_1
2001	12	8	−63.5236	−52.0093	0.792	1	1.167	1	0.375	8069_1
2001	12	8	−63.5023	−52.014	0.819	1	1.167	1	0.347	8069_1
2001	12	8	−63.4961	−51.9741	0.737	1	0.887	3	0.150	8069_1
2001	12	9	−63.5217	−51.8534	0.953	1	0.903	2	−0.049	8069_1
2001	12	9	−63.5365	−51.7021	1.834	1	0.903	2	−0.930	8069_1
2001	12	9	−63.536	−51.659	1.834	1	0.940	1	−0.893	8069_1
2001	12	10	−63.5381	−51.6088	1.834	1	0.940	1	−0.893	8069_1
2001	12	10	−63.5366	−51.5591	0.294	1	0.940	1	0.647	8069_1
2001	12	10	−63.5273	−51.5377	0.294	1	1.156	2	0.863	8069_1
2001	12	10	−63.5233	−51.5031	1.190	1	1.156	2	−0.033	8069_1
2001	12	10	−63.5197	−51.4496	1.190	1	1.138	2	−0.051	8069_1
2001	12	11	−63.4753	−51.3373	0.422	1	0.941	1	0.520	8069_1
2001	12	12	−63.4801	−51.2617	0.782	1	0.941	1	0.159	8069_1
2001	12	12	−63.5044	−51.2427	0.285	1	0.468	1	0.183	8069_1
2001	12	13	−63.5953	−51.1841	0.244	2	0.896	2	0.653	8069_1
2001	12	14	−63.644	−51.1029	0.243	3	1.211	1	0.968	8069_1
2001	12	14	−63.6519	−51.0439	0.308	1	0.704	1	0.396	8069_1
2001	12	14	−63.6913	−50.9159	0.324	1	1.049	1	0.724	8069_1
2001	12	17	−63.6962	−50.3407	1.722	1	1.324	1	−0.398	8069_1
2001	12	18	−63.6926	−50.2376	1.722	1	1.324	1	−0.398	8069_1
2001	12	20	−63.7059	−49.9768	1.791	2	0.821	1	−0.970	8069_1
2001	12	23	−63.7198	−49.5904	0.725	1	0.729	1	0.004	8069_1
2001	12	31	−63.7825	−48.7228	0.549	1	0.271	1	−0.278	8069_1
2002	1	6	−63.8292	−48.0161	0.224	1	0.190	1	−0.034	8069_1
2002	1	6	−63.8281	−47.976	0.188	1	0.190	1	0.002	8069_1
2002	2	12	−64.1033	−46.9666	0.155	1	0.174	1	0.019	8069_1
2002	2	13	−64.1451	−46.8456	0.155	1	0.174	1	0.019	8069_1
2002	2	7	−68.456	−5.043	0.334	1	0.313	1	−0.021	9366_4

Table 1 (*continued*)

Year	Month	Day	Latitude	Longitude	Before iceberg transit		After iceberg transit		Δchl^i	Iceberg tag
					$\langle chl^i_{before}\rangle$	No. obs.	$\langle chl^i_{after}\rangle$	No. obs.		
2003	12	7	−70.8159	−10.858	0.105	2	0.176	1	0.070	9370_6
2004	2	14	−73.7743	−34.2745	0.344	1	0.300	1	−0.045	9370_6
2000	2	24	−66.3808	17.1785	0.165	1	0.228	1	0.062	9372_2
2001	1	10	−53.8331	53.07	0.270	1	0.439	1	0.169	9667_1
2000	10	1	−58.2018	−42.097	0.149	1	0.174	1	0.026	9781_1
2000	2	15	−65.1955	−41.9513	0.147	1	0.112	1	−0.035	9782_1
2000	3	23	−65.108	−41.1603	0.111	2	0.058	1	−0.053	9782_1
2000	3	25	−65.1203	−40.9207	0.089	2	0.055	1	−0.034	9782_1
2000	10	10	−55.197	−23.287	0.188	1	0.113	1	−0.075	9782_1
2002	2	27	−58.9218	18.8978	0.152	1	0.219	1	0.067	9803_2
2003	3	9	−53.624	−33.187	0.289	1	0.303	1	0.014	9831_4
2003	3	10	−53.591	−33.092	0.200	1	0.336	1	0.135	9831_4
2000	3	26	−65.7041	−42.1808	0.103	1	0.121	1	0.018	9834_1

Table 2
Statistical results for the cases where a tracked iceberg was and was not present.

	Δchl^i	Δchl^{ni}	Δchl^i and Δchl^{ni} sig. different?
All data			
No. datapoints	215	690444	
Median ± std. deviation	0.0808 ± 1.5208	0.0100 ± 2.0844	Yes ($p<1\times10^{-6}$)
Normal? (Barque-Jera test)	No ($p<0.001$)	No ($p<0.001$)	
Normal $\Delta chl = \log(\langle chl^i_{before}\rangle) - \log(\langle chl^i_{before}\rangle)$? (Barque-Jera test)	No ($p<0.001$)	No ($p<0.001$)	
Skewness	1.1340	−1.4768	
Monthly data			
	Δchl^i Median ± std. dev.	Δchl^{ni} Median ± std. dev.	Δchl^i and Δchl^{ni} sig. different?
October	0.0273 ± 0.0464 $N=20$	0.0209 ± 0.3370 $N=42732$	No ($p=0.28$)
November	0.2165 ± 0.7018 $N=51$	0.0661 ± 0.9875 $N=86925$	Yes ($p<1\times10^{-3}$)
December	0.1865 ± 2.7340 $N=43$	0.0098 ± 2.6954 $N=140578$	Yes ($p=0.0086$)
January	0.1003 ± 0.7074 $N=59$	0.0055 ± 1.9003 $N=147454$	Yes ($p=0.003$)
February	−0.0012 ± 1.8282 $N=34$	0.0093 ± 2.6493 $N=178964$	No ($p=0.45$)
March	0.0161 ± 0.0944 $N=8$	−0.0123 ± 0.8828 $N=77857$	No ($p=0.47$)

Significant differences were assessed using the Mann-Whitney-Wilcoxon test, and *p*-values are given.

iceberg passage, initial chlorophyll values, $\langle chl_{before}\rangle$, were considered in detail (see Table 3). The median values of chlorophyll prior to a known iceberg transit, $\langle chl^i_{before}\rangle$, were 0.39 mg m^{-3} in the case that chlorophyll subsequently increased, compared to 0.60 mg m^{-3} when chlorophyll subsequently decreased. The median initial values of chlorophyll when no tracked iceberg was passing, $\langle chl^{ni}_{before}\rangle$, were 0.32 mg m^{-3} in the case that chlorophyll subsequently increased, compared to 0.53 mg m^{-3} when chlorophyll subsequently decreased. For both $\langle chl^i_{before}\rangle$ and $\langle chl^{ni}_{before}\rangle$, the positive and negative cases were significantly different according to the Mann-Whitney-Wilcoxon test ($p \ll 0.01$, $N=215$ and 690,444, respectively). This implies that the sign of the effect that a given iceberg had on chlorophyll (positive/negative) was influenced by initial chlorophyll conditions. Breaking these data down by month (see Table 3) showed that median $\langle chl^i_{before}\rangle$ values were significantly different only from October to December, i.e. during spring and not summer. The October case was of significant difference between 0.1477 mg m^{-3} (subsequent increase in chl) and 0.1523 mg m^{-3} (subsequent decrease in chl), with only 5 instances of a subsequent decrease compared to 15 instances of a subsequent increase. The similarity between $\langle chl^i_{before}\rangle$ and $\langle chl^{ni}_{before}\rangle$ suggests that a larger dataset for $\langle chl^i_{before}\rangle$ might be required in order to detect, statistically, the effect of differing initial conditions for each month (i.e. we have a type I error). Median $\langle chl^i_{before}\rangle$ values were also very similar for positive and negative Δchl^i during November and January, but only during October and March for the background dataset. Most strikingly, during December median $\langle chl^i_{before}\rangle$

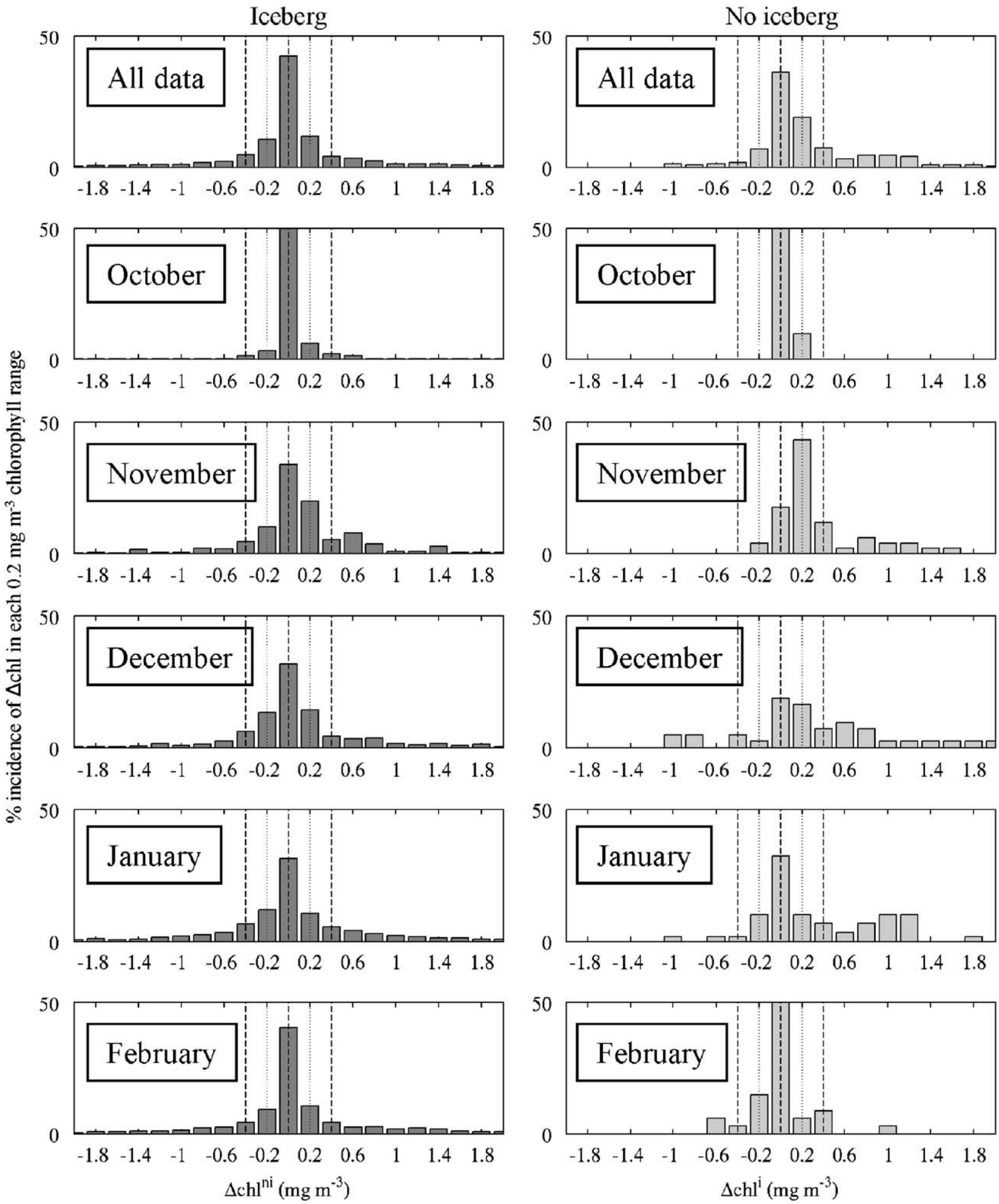

Fig. 2. Frequency distributions of Δchl^{ni} (left-hand column) and Δchl^{i} (right-hand column) values, for the full dataset and for individual months. The histograms were generated using Δchl intervals of 0.2 mg m^{-3}, with the middle bin centred at 0 (i.e. $\Delta chl = \pm 0.1$ mg m^{-3}). To aid interpretation, dashed lines indicate the centre of the central bin and of those centred at ± 0.4 mg m^{-3}, and dotted lines indicated the centre of the bins at 0.2 mg m^{-3}.

values were much higher prior to a negative Δchl^{i} event, and there are no similar cases for the background dataset. This confirms that where an iceberg transits a well-developed bloom with high surface chlorophyll concentrations in the late spring/early summer, its immediate impact is likely to be a reduction in surface chlorophyll

Table 3
Initial 6-day mean surface chlorophyll concentrations, $\langle chl^{i}_{before} \rangle$, prior to a known iceberg transit and for the background dataset where no tracked iceberg transited a given pixel, $\langle chl^{ni}_{before} \rangle$, summarised for cases where the change in chlorophyll was positive and negative.

Data period	Iceberg			No iceberg		
	$\langle chl^{i}_{before} \rangle$			$\langle chl^{ni}_{before} \rangle$		
	$\Delta chl^{i} > 0$	$\Delta chl^{i} < 0$	Significant difference? $\alpha = 0.01$	$\Delta chl^{ni} > 0$	$\Delta chl^{ni} < 0$	Significant difference? $\alpha = 0.01$
All data	0.39	0.60	Y ($p \sim 0$)	0.32	0.53	Y ($p \sim 0$)
October	0.15	0.15	Y ($p = 0.02$)	0.15	0.18	Y ($p \sim 0$)
November	0.43	0.54	Y ($p = 0.001$)	0.30	0.59	Y ($p \sim 0$)
December	0.77	1.72	Y ($p < 1 \times 10^{-5}$)	0.36	0.73	Y ($p \sim 0$)
January	0.57	0.60	N ($p = 0.62$)	0.56	0.91	Y ($p \sim 0$)
February	0.31	0.47	N ($p = 0.20$)	0.39	0.59	Y ($p \sim 0$)
March	0.20	0.11	N ($p = 0.57$)	0.22	0.30	Y ($p \sim 0$)

Significance was assessed using the Mann-Whitney-Wilcoxon test, with $\alpha = 0.01$.

Table 4
Probabilities of an iceberg transit resulting in an increase in surface 6-day mean chlorophyll concentration.

Seasonal subset	Iceberg					No iceberg					Increase in P_{inc} attributed to iceberg =
	Med (chl^{i}_{bef})	$N^{i}_{tot} = A$	$N[\Delta chl^{i} > 0] = B$	$N[\Delta chl^{i} < 0] = C$	$P^{i}_{inc}Q = B/A$	Med(chl^{ni}_{bef})	$N^{ni}_{tot} = X$	$N[\Delta chl^{ni} > 0] = Y$	$N[\Delta chl^{ni} < 0] = Z$	$P^{ni}_{inc}R = Y/X$	$100(Q-R)/R$ (%)
All	0.46	215	147	68	0.68	0.39	690,444	371,825	318,618	0.54	26
October	0.15	20	15	5	0.75	0.15	42,732	28,339	14,393	0.66	14
November	0.46	51	46	5	0.90	0.33	86,981	57,750	29,231	0.66	36
December	0.96	43	30	13	0.70	0.49	142,489	74,929	67,560	0.53	32
January	0.59	59	34	25	0.58	0.67	148,129	76,324	71,804	0.48	21
February	0.34	34	17	17	0.50	0.44	181,003	94,678	86,325	0.52	−4
March	*0.18*	*8*	*5*	*3*	*0.63*	0.26	77,907	34,031	43,876	0.44	*43*

P denotes probability, superscripts i and ni stand for 'iceberg' and 'no iceberg', *N* denotes number of data points. Capitals *A–C*, *X–Z*, *Q* and *R* are defined within the table to clarify the probability calculations. Figures for March are italicized to stress the low number of match-up points in this month.

concentration. However, there were only 13 such cases during December, compared to 30 cases of an iceberg encountering lower 6-day mean chlorophyll concentrations with a subsequent increase in chlorophyll.

Table 4 gives a summary of the positive and negative Δchl results for easy comparison of the cases with and without iceberg transit. Δchl^{i} was positive in 147 of the 215 transit events detected, and negative in 68 cases. In contrast, Δchl^{ni} was positive in 371,825 cases, negative in 318,618 cases. These figures can be expressed as the probability of finding an increase in surface chlorophyll after the iceberg transit using the expression

$$P^{i}_{inc} = N[\Delta chl^{i} > 0]/N^{tot} \quad (3)$$

where *P* denotes the probability, $N[\Delta chl^{i} > 0]$ denotes the number of events in which Δchl^{i} was positive and N^{tot} denotes the total number of match-up events ($N^{tot} = 215$). Similarly, for the background case of no iceberg transit:

$$P^{ni}_{inc} = N[\Delta chl^{ni} > 0]/N^{tot}_{ni} \quad (4)$$

For the background dataset, increases in 6-day mean surface chlorophyll occurred in 44–66% of cases per month, with the greatest chances of an increase during October and November, and the lowest chance of an increase during March. A decrease in surface chlorophyll was more likely than an increase during January and March. With a tracked iceberg transit, the probability of an increase was higher than the background case for every month except February, with probabilities ranging from 50% (February) to 90% (November). Taking a direct comparison of these probabilities for the background and iceberg transit datasets, the presence of an iceberg increased the likelihood that surface chlorophyll would increase between adjacent 6-day periods by between −4% and 43% (see final column of Table 4), with negative values occurring only during February. As discussed previously, it is likely that the February results can be attributed to dilution of surface chlorophyll under conditions of strong and shallow stratification as the iceberg stirs up water from below the mixed layer.

To explore whether particular locations were associated with an increased chance of positive or negative iceberg impacts, values of Δchl were mapped (Fig. 3). For known iceberg transit sites, more positive incidents were grouped around the South Orkney and South Georgia islands and toward East Antarctica, while mostly negative values were found in the location of the Weddell Gyre. The cluster of data around the Antarctic Peninsula represents a balanced mix of positive and negative iceberg impacts. For the background data, positive and negative Δchl^{ni} values were found all along the iceberg paths. Fig. 3b also

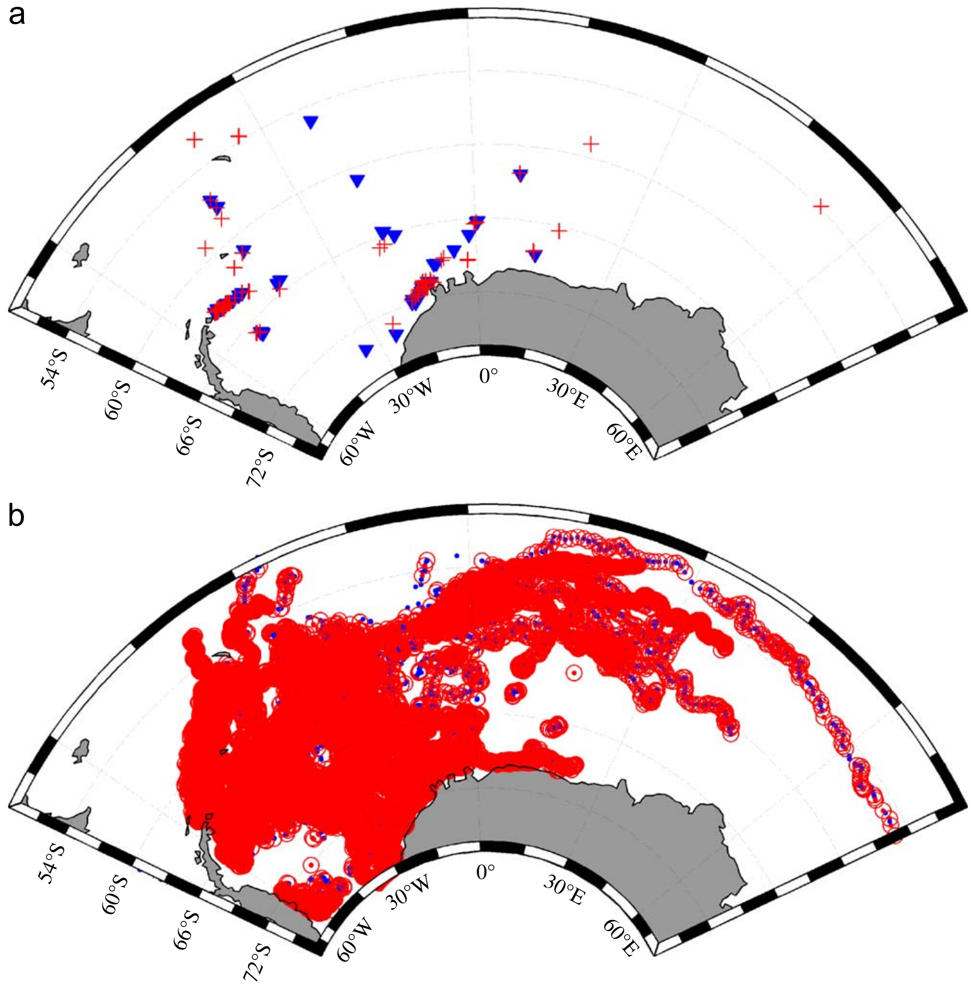

Fig. 3. (a) Locations at which a negative change in 6-day mean surface chlorophyll after the passage of a tracked iceberg was recorded: $\Delta chl^{i} < 0\,mg\,m^{-3}$ (blue down-arrows) and at which a positive change in chlorophyll after the passage of a tracked iceberg was recorded: $\Delta chl^{i} > 0\,mg\,m^{-3}$ (red plus-signs). (b) As in (a) but for the background dataset, where no tracked iceberg transited each pixel.

illustrates the extent of the tracked iceberg dataset, which covers most of the Weddell Sea and stretches more sparsely some tens of degrees to the east in the central Southern Ocean.

This study is influenced by the seasonality of the SeaWiFS record: As a passive instrument detecting sunlight that is scattered out of the ocean, there are no measurements during cloudy periods, or when sea-ice cover is present, or during the dark winter months. The satellite signal also originates from varying depths, depending on the turbidity of the water: Although it has been shown that the algorithms used to derive chlorophyll are generally sound when compared with surface samples analysed using high performance liquid chromatography (Marrari et al., 2006), the satellite may not detect deep chlorophyll maxima which are common in the Southern Ocean (e.g. Holm-Hansen and Hewes, 2004). Confirmation of the results therefore requires a considerable *in situ* sampling effort. However, under clear satellite viewing conditions the comparison between the iceberg and background datasets presented here yields a valid assessment of iceberg impacts on satellite-derived surface chlorophyll, because the only factor differing between the two datasets is the presence or absence of a tracked iceberg.

It is a significant limitation of this study that only short-term chlorophyll fluctuations can reasonably be studied. In order to gauge the longer-term effect of drifting icebergs on the productivity of the Southern Ocean, a dataset detailing total numbers of icebergs over a number of years needs to be compared with the large-scale biomass or productivity of the region, yielding insight into whether years in which more icebergs calved are generally more or less productive. This goal will not be met until realistic annual estimates of iceberg numbers (and volume) can be produced, perhaps by applying automated iceberg tracking to visible, microwave and radar remote-sensing data. *In situ* data would also be required in such a study to validate both the iceberg tracking and the productivity algorithms.

4. Conclusions

For the period October through to February the impact of icebergs on surface chlorophyll has been shown to be a net, statistically significant, increase exceeding ambient biomass fluctuations. This is particularly significant for the common iceberg drift paths which have been identified so far as following the Antarctic coastal current westwards and transiting north via gyre circulations at numerous locations, into the eastward flowing Antarctic Circumpolar Current (ACC) (Schodlok et al., 2006; Gladstone et al., 2001). If borne out by *in situ* evidence, these results indicate that differences in phytoplankton activity between glacial and inter-glacial periods may have been influenced by iceberg numbers and distributions, and that any future change in calving patterns may affect phytoplankton growth, and thereby carbon sequestration, in the Southern ocean.

On a more speculative note, these iceberg drift paths represent large swaths into which phytoplankton are transported via the island sanctuary of an iceberg (Smith et al., 2007), far from their coastal origins. Strong latitudinal gradients across the Southern Ocean, associated with the ACC, limit the south-north advection of phytoplankton cells. Transport of cells upon icebergs therefore represents an extremely efficient and unique means of bringing cold-adapted, Antarctic coastal phytoplankton northwards (and simultaneously modifying local conditions, if only briefly, to favour growth), perpetually replenishing species diversity, and this may explain why the dominant phytoplankton species in the ACC frontal systems vary dramatically from year to year.

According to the results presented here, the logistical and financial cost associated with detailed *in situ* studies of iceberg colonisation and progress from the coastal current into open waters are certainly justified.

Acknowledgements

We thank Heike Losch, Martin Losch, Christoph Voelker and Victor Smetacek for helpful discussions and comments on the manuscript and Thomas Busche for programming assistance in the preliminary data analysis. We also thank two anonymous reviewers for their constructive and insightful comments. Level 2 chlorophyll data were kindly provided by the NASA SeaWiFS Project. MODIS-Aqua images were provided by the NASA MODIS Science Team Level 1 and Atmosphere Archive and Distribution System. This paper is dedicated to pilot Stefan Winter who assisted with deployment of the iceberg tracking devices and sadly passed away in Antarctica in March, 2008.

References

Arrigo, K.R., van Dijken, G.L., Ainley, D.G., Fahnestock, M.A., Markus, T., 2002. Ecological impact of a large Antarctic iceberg. Geophysical Research Letters 29 (7).

Bailey, S.W., Werdell, P.J., 2006. A multi-sensor approach for the on-orbit validation of ocean color satellite data products. Remote Sensing of Environment 102 (1–2), 12–23.

Campbell, J.W., 1995. The lognormal-distribution as a model for bio-optical variability in the sea. Journal of Geophysical Research—Oceans 100 (C7), 13237–13254.

Dafner, E., Mordasova, N., Arzhanova, N., Maslennikov, V., Mikhailovsky, Y., Naletova, I., Sapozhnikov, V., Selin, P., Zubarevich, V., 2003. Major nutrients and dissolved oxygen as indicators of the frontal zones in the Atlantic sector of the Southern Ocean. Journal of Geophysical Research 108 (C7).

de Baar, H.J.W., 1995. Importance of iron for phytoplankton blooms and carbon-dioxide drawdown in the Southern-Ocean. Nature 373, 412.

de Baar, H.J.W., de Jong, J.T.M., Nolting, R.F., Timmermans, K.R., van Leeuwe, M.A., Bathmann, U., van der Loeff, M.R., Sildam, J., 1999. Low dissolved Fe and the absence of diatom blooms in remote Pacific waters of the Southern Ocean. Marine Chemistry 66 (1–2), 1–34.

Dowdeswell, J.A., Bamber, J.L., 2007. Keel depths of modern Antarctic icebergs and implications for sea-floor scouring in the geological record. Marine Geology 243, 120–131.

Edwards, R., Sedwick, P., Morgan, V., Boutron, C., 2006. Iron in ice cores from Law Dome: a record of atmospheric iron deposition for maritime East Antarctic during the Holocene and Last Glacial Maximum. Geochemistry, Geophysics, Geosystems 7 (12).

Gladstone, R.M., Bigg, G.R., Nicholls, K.W., 2001. Iceberg trajectory modelling and meltwater injection in the Southern Ocean. Journal of Geophysical Research 106 (C9), 19,903–19,915.

Gordon, H.R., McCluney, W.R., 1975. Estimation of the depth of sunlight penetration in the sea for remote sensing. Applied Optics 14, 413–416.

Hill, V.J., Matrai, P., Olsen, E., Zimmerman, R., 2008. The influence of sea ice on Arctic Ocean marine primary production: regional responses. In: Proceedings of Ocean Optics Conference XIX, Barga-Gallicano, Italy.

Holm-Hansen, O., Hewes, C.D., 2004. Deep chlorophyll-a maxima (DCMs) in Antarctic Waters. Polar Biology 27, 699–710.

Huppert, H.E., 1980. The physical processes involved in the melting of icebergs. Annals of Glaciology 1, 97–101.

Jansen, D., Schodlok, M.P., Rack, W., 2007. Basal melting of A-38B: a physical model constrained by satellite observations. Remote Sensing of Environment 111, 195–203.

Jenkins, A., 1999. The impact of melting ice on ocean waters. Journal of Physical Oceanography 29, 2370–2381.

Lancelot, C., Mathot, S., Veth, C., de Baar, H., 1993. Factors controlling phytoplankton ice-edge blooms in the marginal ice-zone of the northwestern Weddell Sea during sea ice retreat 1988: field observations and mathematical modelling. Polar Biology 13, 377–387.

Lannuzel, D., Schoemann, V., De Jong, J., Tison, J.-L., Chou, L., 2007. Distribution and biogeochemical behaviour of iron in the East Antarctic sea ice. Marine Chemistry 106, 18–32.

Lyons, L., 1991. A Practical Guide to Data Analysis for Physical Science Students. Cambridge University Press, Cambridge.

Marrari, M., Hu, C., Daly, K., 2006. Validation of SeaWiFS chlorophyll a concentrations in the Southern Ocean: a revisit. Remote Sensing of Environment 105, 367–375.

Martin, J.H., Gordon, R.M., Fitzwater, S.E., 1991. The case for iron. Limnology and Oceanography 36, 1793–1802.

Mitchell, B.G., Holm-Hansen, O., 1991. Observations and modelling of the Antarctic phytoplankton crop in relationship to mixing depth. Deep-Sea Research 38A (8), 981–1008.

Morel, A., Berthon, J.F., 1989. Surface pigments, algal biomass profiles, and potential production of the euphotic layer: relationships reinvestigated in view of remote-sensing applications. Limnology and Oceanography 34 (8), 1545–1562.

O'Reilly, J.E., Maritorena, S., Mitchell, B.G., Siegel, D.A., Carder, K.L., Garver, S.A., Kahru, M., McClain, C., 1998. Ocean color chlorophyll algorithms for SeaWiFS. Journal of Geophysical Research—Oceans 103 (C11), 24937–24953.

Sachs, O., 2008. Personal communication.

Schodlok, M.P., Hellmer, H.H., Rohardt., G., Fahrbach, E., 2006. Weddell Sea iceberg drift: five years of observations. Journal of Geophysical Research 111, C06018.

Smetacek, V., Klaas, C., Menden-Dever, S., Ryanearson, T.A., 2002. Mesoscale distribution of dominant phytoplankton species relative to the hydrographical field along the Antarctic Polar Front. Deep-Sea Research II 49, 3835–3848.

Smith Jr., K.L., Robison, B.H., Helly, J.J., Kaufmann, R.S., Ruhl, H.A., Shaw, T.J., Twining, B.S., Vernet, M., 2007. Free-drifting icebergs: hot spots

of chemical and biological enrichment in the Weddell Sea. Science 317, 478–482.
Smith, W.O., 1985. Phytoplankton bloom produced by a receding ice edge in the Ross Sea—spatial coherence with the density field. Science 227, 163.
Smith, W.O., Comiso, J.J., 2008. Influence of sea ice on primary production in the Southern Ocean: a satellite perspective. Journal of Geophysical Research 113 (C5) Article No. C05S93.
Sullivan, C.W., Arrigo, K.R., McClain, C.R., Comiso, J.C., Firestone, J., 1993. Distributions of phytoplankton blooms in the Southern Ocean. Science 262, 1832–1837.
Uitz, J., Claustre, H., Morel, A., Hooker, S.B., 2006. Vertical distribution of phytoplankton communities in open ocean: an assessment based on surface chlorophyll. Journal of Geophysical Research—Oceans 111 (C8) Article No. C080005.